WHC-SA-2865-FP

Early Containment of High-Alkaline Solution Simulating Low-Level Radioactive Waste Stream in Clay-Bearing Blended Cement

Albert A. Kruger

Date Published
April 1995

To Be Published in
Journal of Hazardous Waste

Prepared for the U.S. Department of Energy
Office of Environmental Restoration and
Waste Management

Westinghouse Hanford Company
P.O Box 1970
Richland, Washington

Hanford Operations and Engineering Contractor for the
U.S. Department of Energy under Contract DE-AC06-87RL10930

Approved for Public Release

DISCLAIMER

Portions of this document may be illegible in electronic image products. Images are produced from the best available original document.

EARLY CONTAINMENT OF HIGH-ALKALINE SOLUTION SIMULATING LOW-LEVEL RADIOACTIVE WASTE STREAM IN BLENDED CEMENT

R.A. Olson, P.D. Tennis, D. Bonen[1], H.M. Jennings, T.O. Mason, B.J Christensen, A.R. Brough*, G.K. Sun* and J.F Young*; Center for Advanced Cement-Based Materials, Northwestern University, 2145 Sheridan Rd., Evanston, IL 60208, *Center for Advanced Cement-Based Materials, University of Illinois at Urbana-Champaign, 204 Ceramics Building, 105 S. Goodwin, Urbana, IL 61801

ABSTRACT

Portland cement blended with fly ash and attapulgite clay was mixed with high-alkaline solution simulating low-level radioactive waste stream at a one-to-one weight ratio. Mixtures were adiabatically and isothermally cured at various temperatures and analyzed for phase composition, total alkalinity, pore solution chemistry, and transport properties as measured by impedance spectroscopy.

The total alkalinity is characterized by two main drops. The early one corresponds to a rapid removal of phosphorous, aluminum, sodium, and to a lesser extent potassium from the pore solution. The second drop from about 10 h to 3 days is mainly associated with the removal of aluminum, silicon, and sodium. Thereafter, the total alkalinity continues descending, but at a lower rate.

All pastes display a rapid flow loss that is attributed to an early precipitation of hydrated products. Hemicarbonate appears as early as one hour after mixing and is probably followed by

---

[1] Communicating author.

apatite precipitation. However, the former is unstable and decomposes at a rate that is inversely related to the curing temperature. At high temperatures, zeolite appears at about 10 h after mixing. At 30 days, the stabilized crystalline composition includes zeolite, apatite and other minor amounts of $CaCO_3$, quartz, and monosulfate.

Impedance spectra conform with the chemical and mineralogical data. The normalized conductivity of the pastes shows an early drop, which is followed by a main decrease from about 12 h to three days. At three days, the permeability of the cement-based waste as calculated by Katz-Thompson equation is over three orders of magnitude lower than that of ordinary portland cement paste. However, a further decrease in the calculated permeability is questionable. It appears that this cement-based waste provides a rapid stabilization/solidification and its 3-day physical containment of the waste is comparable to that of 28-day plain portland cement paste. In addition, chemical stabilization is favorable through incorporation of waste species into apatite and zeolite.

INTRODUCTION

Stabilization/solidification of hazardous waste has become a major concern in the modern industrial society due to the growing public awareness coupled with restrictive environmental regulations governing waste disposal. Cement-based systems are favorable for waste containment because they are considered as durable, inexpensive, nonflammable, set at ambient conditions and have low permeability.

Immobilization of waste in cement-based materials is related to three mechanisms, (a) physical containment, (b) absorption or chemisorption of cations on the large surface area of the paste, and (c) chemical fixation through deposition and ion substitution [1,2]. Mature portland cement paste has a large B.E.T. surface area (about 200 m^2/g as measured by nitrogen) which is attributed to the tortuous and interconnected ink-bottle pores that decrease the transport properties of the paste. Blended cement (e.g., cement containing pozzolanic materials) pastes usually display lower permeabilities than do plain portland cement paste [e.g., 3]. The high pH of about 13.5 to 12.5 characteristic to cement paste is favorable for precipitation of many hazardous metals as hydroxides, such as, cadmium and nickel [1], sulfate, sulfide, phosphate, carbonate [2], and americium [4].

During the recent years, considerable research efforts have been aimed at formulating blended cement for immobilization of low-level radioactive waste. Accordingly, a specific mixture design was developed for the containment of Hanford low-level waste. In a decreasing order, this is based on fly ash, portland cement, and clay needed for meeting high temperatures on one hand, and a wide range of specifications concerning pumpability, toxicity, compressive strength, heat of hydration, leachability, irradiation, thermal conductivity, curing time, and expansion on the other hand [5]. Recent studies conducted on similar blends have shown a rapid setting and precipitation of zeolite as one of the hydrated products [6]. Zeolites are hydrous aluminosilicates that may facilitate a greater rate of chemical fixation due to their high capability of ion exchange.

As a part of a larger research effort aimed at validating the suitability of stabilizing the volatile materials from off-gas system of Low-Level Waste Disposal Vitrification Facility, this blend for immobilizing this kind of waste, the objectives of this paper are to characterize the cement-based waste system and evaluate its transport properties, i.e., the decrease in diffusivity and permeability over time as monitored by impedance spectroscopy.

CONCEPTS OF IMPEDANCE SPECTROSCOPY

Impedance spectroscopy (IS) is an non-destructive electrical analysis technique that has been in use for characterizing the microstructure of cement paste for several years [7-11]. An alternating current is applied to the specimen and the impedance is measured as a function of frequency, which is used to calculate the conductivity and dielectric constant of the paste.

The concentration of the pore solution changes with time, so the conductivity of the paste is normalized by the pore fluid conductivity. The normalized conductivity (σ/σ_0) is a microstructural parameter that is dependent on the size, tortuosity, and interconnectivity of the pores of the paste and defined as:

$$\sigma/\sigma_0 = \Phi_0\beta \qquad (1)$$

where σ = conductivity of the paste , σ_0 = conductivity of the pore fluid, Φ_0 = volume fraction of capillary porosity, and β = a connectivity factor [8,12]. The normalized conductivity decreases with time as the pore volume decreases and the tortuosity increases.

The normalized conductivity of the paste is directly related to the normalized diffusivity through the Nernst-Einstein equation:

$$D / D_0 = (\sigma/\sigma_0) \qquad (2)$$

where D is the diffusivity of the ion in the paste (m^2/s) and D_0 is the intrinsic diffusivity in pure water [8,13]. The normalized conductivity is also related to permeability by the Katz-Thompson equation:

$$K = (1/226) (d_c)^2 (\sigma/\sigma_0) \qquad (3)$$

in which, d_c is the critical pore diameter and K is the permeability (m/sec) [12, 14]. Recently, a reasonable agreement between the permeability derived from IS measurements and values measured by conventional techniques was established [8].

Additionally, the microstructure of the cement paste can also be characterized by its dielectric response. The distribution of pore sizes and the pore structure creates a characteristic dielectric constant (ε) that can reach extremely high values. Assume a material of thickness b is placed between two plates of a capacitor with a separation D and the space between each plate and the material is d. Then the capacitance is defined:

$$C = \varepsilon_{eff}\, \varepsilon_0 (A/D) = \varepsilon_s\, \varepsilon_0 (A/(D-b) = \varepsilon_s\, \varepsilon_0 (A/d) = \varepsilon_s\, \varepsilon_0 (D/d)(A/D) \qquad (4)$$

where ε_{eff} is the effective dielectric constant, ε_s is the dielectric constant of the material in the gap (d), ε_0 is the permittivity of free space, and A is the area of the electrodes. The effective dielectric constant is then:

$$\varepsilon_{eff} = \varepsilon_s \, \varepsilon_0 \, (D/d) \qquad (5)$$

which can be quite large depending upon the D/d ratio, referred to as the dielectric amplification factor. A large amplification and large effective dielectric constants can be obtained if conductive grains with D diameter are embedded in insulating grain boundaries, where d denotes the grain boundary thickness [15]. Based on measurements and modelling, it was suggested that in cement paste the dielectric amplification factor is defined by the capillary pore size (D) and d is the thickness of C-S-H gel between pores [8-11].

EXPERIMENTAL PROCEDURE

To be reiterated, the formulation of the blended cement was carried out elsewhere [5]. One thousand g of dry blended cement composed of 21% ASTM Type I/II portland cement, 68% Class F fly ash, and 11% attapulgite (palygorskite-type) by mass was prepared by rotating it in a large plastic cylinder for 16 h. In parallel, a simulated waste solution with a composition shown in Table 1 was constantly stirred and kept at 50 C. In order to simulate the temperature profile of the industrial waste, the cement was added to the solution when the temperature of the latter

dropped to 45 C. The cement was mixed with the solution at a one-to-one weight ratio in an Hobart mixer for two minutes, stopping twice to redistribute and recover the paste from the walls with a spatula.

In order to analyze the effects of the curing conditions and the various properties of the blend that is supposed to be placed in near-subsurface vaults, four curing regimes were tested. Figure 1 shows the temperature schedule of the samples. The upper curve (sample 4) represents the temperature profile of the blend cured under simulated adiabatic conditions assuming that the maximum temperature goes up to 90 C after 3 days and then level off. The rest (samples 1,2,3) followed the adiabatic conditions up to 55, 70, and 85 C, and then cured isothermally at the corresponding temperatures.

The impedance was measured using a Hewlett-Packard Model 4192A impedance analyzer (Hewlett-Packard, Boulder, CO). An impedance curve was generated by collecting 128 data points in logarithmic intervals in a frequency range of 11 MHz to 5 Hz. The resistance and capacitance of each sample were determined by fitting simulated impedance curves to the experimental curve through the origin [16]. Further details of the measurement and correction processes are given elsewhere [8-10].

A 3 mm thick polycarbonate cylinder with an inner diameter of 23 mm was used as a sample holder for the IS analyses. Two stainless steel electrodes were placed 6 cm apart inside the cylinder. The paste was cast, sealed, and placed horizontally in a glass chamber containing a small amount of de-ionized water to prevent evaporation.

Pore solutions were extracted from companion samples using a steel die press following the procedure of Barneyback and Diamond [17]. The conductivity of the extracted pore solution was measured at the temperature corresponding to the time it was expressed from the paste. Thermal equilibrium was assumed when the conductivity of the solution was constant at 100 kHz. The extracted pore solutions were diluted to 1:100 and analyzed by inductively coupled plasma photospectrometry (Plasma 40, Perkin-Elmer, Norwalk, CT). Additionally, the diluted pore solutions were titrated by adding 0.5 M HNO_3 and measuring the pH change with a digital pH meter. X-ray diffraction (XRD) analyses were carried out in a Phillips diffractometer equipped with a graphite monochrometor.

Mercury intrusion porosimetry measurements (MIP) were conducted using a Quantachrome Autoscan 33, pressurizing from ambient to 33000 psi. Samples were solvent replaced with methanol for 1 day, then D-dried for at least 2 days before testing. The critical pore diameter was defined as the inflection point in the total intruded volume vs. diameter curve (the maximum dV/dP value).

Table 1: Chemical Composition of the Simulated Waste

Compound	Amount (g/l)	Molecular Weight	Density (g/cc)
$NaNO_3$	8.58	84.99	2.26
NaOH (50%)	149.7	40.00	2.13
$Al(NO_3)_3 \cdot 9H_2O$	128	375.13	
$Na_3(PO4) \cdot 12H_20$	74.4	380.12	1.62
$NaNO_2$	36.9	69.00	2.17
$Na2CO_3$	36.2	105.99	2.53
KCl	1.83	74.56	1.98
NaCl	2.5	58.44	2.17
$Na_3(C_6H_5O_7) \cdot 2H_2O$	2.5	294.10	
$Na_2B_4O_7$	0.131	201.22	2.37
Na_2SO_4	3.89	142.04	2.68
$Ni(NO_3)_2 \cdot 6H_2O$	0.302	290.81	2.05
$Ca(NO_3)_2 \cdot 4H_2O$	0.438	236.15	1.90
$Na_4(EDTA) \cdot 2H_2O$	1.415	416.21	
$Na_3(HEDTA)$	5.293	380.24	
$HOCH_2COOH$	0.645	76.05	
$Mg(NO_3)_2 \cdot 6H_2O$	0.028	256.41	1.64

RESULTS AND DISCUSSION

Total Alkalinity and Pore Solution Composition

Figure 2 shows the titration curves of the pore solutions extracted at various times from the cement-based waste cured adiabatically. The original waste solution displays a step-like curve with several end points corresponding to the neutralization of different species, e.g., OH^-, NO_2^-, NO_3^-, PO_4^{3-}, and CO_2^{2-} (see Table 1). The pore solution extracted at 0.2 h also produces a step-like curve, but its ionic strength is considerably lower than that of the original waste. By one hour and onward, the titration curves are S-shaped with a single end point, indicating that through precipitation OH^- becomes the predominant species governing the pH of the pore fluids. Additionally, attention is drawn to the continuous decrease of the ionic strength of the pore fluids.

Figure 3 shows the decrease of the total alkalinity with time. The term total alkalinity is defined here as the acid neutralizing capacity titrated down to pH 7 and expressed as OH^- equivalent. A substantial drop in the total alkalinity from about 3.9 to 2.5 M occurs from mixing to one hour (Figure 3a), probably due to an early removal of P, Al, Na, and K as is shown below. Thereafter, the monotonic decrease in the total alkalinity is followed by a major drop from about 10 to 100 h. After about 3 days, a further decrease in the total alkalinity is registered, but at a lower rate. The above main drop corresponds to a notable decrease in the pH (Figure 4), and the resultant changes in composition and precipitation of phases bear a significant effect on the impedance spectra.

Pore solutions were measured for sodium, potassium, calcium, silicon, sulfur, aluminum, and phosphorous contents. The latter is almost completely removed from the pore solution within the first four hours from mixing (Figure 5). Aluminum follows a similar course and its concentration in the pore solution decreases more than 5 fold. The rates of removal are inversely related to the curing temperatures. Sodium shows a greater dependence on temperature. At 55 C only a slight decrease in its concentration was recorded, whereas at 90 C, it drops from about 4000 to 2500 mmolar. Potassium also decreases during the first four hours, but at a lower rate. It is evident that any decrease or increase in the pore solution concentration is the result of precipitation or dissolution, respectively. Thus, the concentration of the species in the pore solution is also affected by the solid phases of the blended cement. This means that once phosphorous was removed from the original waste solution there is no other source for it. In contrast, the fly ash and to a lesser extent, the clay provide a continuous supply of silicon, aluminum, and potassium through the decay of the solid constituents.

Figure 6 is an another illustration for the removal of the elements from the pore fluid of the adiabatically cured paste. The second drop in the total alkalinity (Fig. 3) from about 10 h to 3 days corresponds to a decrease of Al^{3+},Si^{4+}, and to a lesser extent of Na^{+} and S^{6+}. Ca^{2+} and K^{+} concentrations have the lowest decrease rates. After 3 days, the rate of removal of ions from the pore solution considerably slows down.

Phase Composition

It should be noted that Hanford tank waste solution has two unfavourable features: high alkalinity and high temperature. The latter is expected to result form the internal heat generated due to the low-level radioactive waste decomposition in the large isolated disposal sites. This in turn gives rise to uncommon hydrated products that are formed in cementitious materials. Brough et al. [6] x-rayed similar pastes cured from 45 to 90 C and showed that tetracalcium aluminate monosulfate (AFm) phase appears in the paste cured at 45 C one hour after mixing and reaches a maximum at one day. At 7 days, its content is about one third of its maximum. In the paste cured adiabatically, it reaches a maximum at 9 h and disappears at 1 day. In the latter paste, zeolite (sodalite-type) appears at 9 h and its content is steadily increased over time. In the paste cured at 45 C, zeolite appears at about 1 day. Katz et al. [18] has noted that a significant amount of heat is liberated during the time corresponding to AFm formation, and this reaction is the main source of heat generated under adiabatic conditions.

In another suites of pastes cured at 55, 70, and 90 C up to 30 days, hemicarbonate (tetracalcium aluminate hemicarbonate-12 hydrate) appears in the one-day x-ray pattern of the specimen cured at 55 C, but is absent from 3 days and on. Figure 7 shows the corresponding peaks for hemicarbonate (H), zeolite (Z), and calcium phosphate (ap) at 1 day and 55 C. In addition, a fair amount of unreacted clinker minerals (alite designated as A), quartz (Q) and mullite (M) are present. The calcium phosphate formed is probably carbonate apatite. However, strong diffractions, especially around its strongest line at about a d-spacing of 2.8 A prevent absolute identification. Nevertheless, the almost complete removal of phosphorous from the pore solution makes the deposition of apatite or another phosphate phase unavoidable. The effects of

age and temperature on the apatite peak-height is questionable. It appears that its peak-height increases to some extent up to 3 days and at higher temperatures, but the latter can equally be related to a better crystallization.

In turn, zeolite formation is clearly age and temperature controlled. Higher temperatures favor a higher rate of zeolite deposition. Figure 8 also shows that the amount of zeolite increases to some extent up to 30 days. Fraay et al. [19] and Bijen et al. [20] indicated that the rate of fly ash dissolution is related to alkalinity, pH, and temperature, and it is quite sluggish below pH 13 and 40 C. It may be postulated, therefore, that the dissolution rate of fly ash slows down with time, as is supported by the moderate increase in peak height of zeolite at 30 days. This may also account for the lack of change in the transport properties after 3 days as is discussed below.

In addition to the phases mentioned, calcite is identifiable from 3 days and onward. At 30 days, besides C-S-H, the stabilized phase assemblage includes zeolite, apatite, quartz, and calcite. Of interest are two more features. The appearance of a small peak of AFm phase at 90 C and the reduction of the mullite peak at about 3.39 A. The former phase probably corresponds to monosulfate and the absence of the latter one may indicate that the crystalline phases of the fly ash have become amorphous. Attention is drawn to the potential chemical fixation of this system, as apatite, zeolite, and monosulfate can incorporate many heavy metals including radioactive ones into their structures.

Impedance Spectroscopy

Figure 9 displays the normalized conductivity vs. time for the above pastes. Although the curing temperature affects the normalized conductivity, the patterns as a whole are similar. At one hour the normalized conductivity drops sharply irrespective of temperature, indicating a rapid formation of products that results in a decrease and/or disconnection of capillary porosity (refer to equation 1). In turn, the normalized conductivity of plain portland cement has higher values and decreases at a lower rate. The rapid decrease of the normalized conductivity of the cement-based waste is also supported by the rapid setting behavior of these pastes. It was noted that a rapid flow loss occurred within the first hour after mixing, which is probably related to the early precipitation of hemicarbonate and apatite.

Several simplified systems were cured isothermally at 85 C for 24 h for evaluating the effects of precipitation on the normalized conductivity. Solutions of NaOH, $Al(NO_8)\cdot 9H_2O$, and $Na_3(PO_4)\cdot 12H_2O$ were mixed with cement and fly ash at 1:1 ratio by mass. It was noticed that the conductivity at one hour does not decrease unless $Na_3(PO_4)\cdot 12H_2O$ is added to the mixtures. This supports the view that phosphate joins hemihydrate and precipitates at one hour, and both phases play a dominant role causing a reduction in the paste consistency and an early set.

Following the early precipitation discussed above, the normalized conductivity of the pastes cured at different conditions continues descending at various rates (Fig. 9). The shoulder that appears after about 3 h may be related to deposition of C-S-H along with the previous phases, and by six hours, the normalized conductivity has reached 0.1, about 25% of its original

value.

The main drop in the normalized conductivity appears after about 12 h. This drop, which is most certainly associated with zeolite formation, effectively reduces the normalized conductivity by reducing the capillary porosity and increasing the tortuosity of the capillary pores. At 24 h, the normalized conductivity is already over an order of magnitude lower than its original starting value.

Permeability

Permeability was calculated via the Katz-Thompson equation (eq. 3) using the measured values of the normalized conductivity and the critical pore diameter. Figure 10 displays the permeability constant (K) for hydration times of 3, 7, 14, 28 days, and 3 months, of the paste cured at 90C, together with calculated values from Christensen et al. [8], and measured values from Nyame and Illston [21, 22], and Banthia and Mindess [23] for portland cement pastes. It appears that at 3 days the permeability of the cement-based waste (waste solution-to solids ratio of 1.0) is over three orders of magnitude lower than that of portland cement paste with a w/c of 0.5, and over an order of magnitude lower than cement paste with a w/c of 0.35. Apparently, the products formed at a few days in the cement-based waste reduce the permeability more effectively than the corresponding plain portland cement pastes. However, between three days and three months the permeability remains constant, probably because zeolite precipitation slowed down due to a decrease in pH. Thus, at 28 days, the permeability of the plain cement is about

the same order of magnitude as the cement-based waste corresponding to the range of 10^{-11} and 10^{-12} m/sec.

Dielectric Amplification

Figure 11 is a plot of the effective dielectric constant vs. time of the specimens cured at 55, 70 and 85 C. The dielectric constant of the latter two specimens begins increasing at the same time, just after the drop in the normalized conductivity at about 10 h suggesting that zeolite induces dielectric amplification. The extremely high dielectric constants recorded correlate to a high D/d ratio. This is interpreted in terms of the presence of large conductive pores embedded in thin boundary layers. To be noted is the decrease in ε with temperature. This may be attributed to the coarser pore structure of portland cement paste cured at higher temperatures [3] suggesting that the paste cured at 55 C has a lower D/d ratio and a more homogeneous microstructure.

In contrast to portland cement, the dielectric constant of the cement-based waste follows a different course. Once a maximum was established (large pores with thin walls) it does not decrease. This supports the view that after about 3 days changes in the pore microstructure are limited.

CONCLUSIONS

(1) Hanford waste is characterized by an early set due to deposition of hemicarbonate and apatite. This results in a sharp depletion of the corresponding ions from the pore solution and a drop of over 66% in the normalized conductivity within the first 4 hours.

(2) The combination of high sodium content and high-Al bearing ingredients at high temperatures facilitates zeolite precipitation as early as ten hours after mixing. This stage is marked by a prominent decrease in the total alkalinity, pH, and normalized conductivity.

(3) The rapid decrease in the normalized conductivity results in a corresponding decrease in permeability. Even though the normalized conductivity does not drop after three days, it is comparable to that of 28-day plain portland cement paste.

(4) The 28-days phase assemblage of the cement-based waste is composed of naturally occurring minerals: zeolite, apatite, quartz, and calcite, along with C-S-H and possible minor amount of monosulfate.

(5) Solidification/stabilization of the waste is attributed to the early physical containment of the waste and potential chemical fixation due to incorporation of elements into the apatite and zeolite structures.

ACKNOWLEDGMENT

This work is supported by Westinghouse Hanford Company, Low-Level Waste Disposal Program The help of Ash Grove Cement Co., Engelhard Co., and Koch Minerals Company, for supplying the materials is highly appreciated.

REFERENCES

1. D. Bonen and S.L. Sarkar, "The Present State-of-the-Art of Immobilization of Hazardous Heavy Metals in Cement-Based Materials," Adv. Cem. Concr., ed. M.W. Grutzeck and S.L. Sarkar, Proceedings of an Engineering Foundation Conference, New Hampshire, Durham, July 24-29, American Society of Civil Engineers, pp. 481-498, 1994.

2. J.R. Conner, Chemical Fixation and Solidification of Hazardous Wastes, Van Nostrand Reinhold, New York (1990).

3. H.F.W. Taylor, Cement Chemistry, Academic Press Ltd., London (1990).

4. R. Ataback, P. Bouniol, P. Vitorge, and P. Lebescop," Cement Use for Radioactive Waste Embedding and Disposal Purposes," Cem. Concr. Res., 22[2/3] 419-429 (1992).

5. R.O. Lokken, P.F.C. Martin and S. E. Palmer, "Effects of Curing Temperature and Curing Time on Double-Shell Tank Waste Grouts", Pacific Northwest Laboratory, HGTP-93-0302-01, August, 1993.

6. A. Brough, A. Katz, T. Bakharev, R.J. Kirkpatrick, L.J. Struble, and J.F. Young, "Microstructural Aspects of Zeolite Formation in Alkali Activated Cement Containing High Levels of Fly Ash," Mat. Res. Soc. Proc., (1994, in press).

7. P. Gu, Z. Xu, P. Xie, and J.J. Beaudoin, "Application of A.C. Impedance Techniques in Studies of Porous Cementitious Materials, (I), (II), and (III). Cem. Concr. Res., Vol. 23[3] 531-40, (1993). Vol. 23[4] 853-862, (1993), Vol. 23[5] 1007-1015 (1993).

8. B.J. Christensen, R.T. Coverdale, R.A. Olson, S.J. Ford, E.J. Garboczi, T.O. Mason, and H.M. Jennings, "Impedance Spectroscopy of Hydrating Cement-Based Materials: Measurement, Interpretation, and Application," J. Am. Cerm. Soc.77(11)2789(1994).

9. R.T. Coverdale, B.J. Christensen, T.O. Mason, H.M. Jennings, E.J. Garboczi, and D.P.

Bentz, "Interpretation of the Impedance Spectroscopy of Cement Paste Via Computer Modelling I Bulk Conductivity and Offset Resistance," J. Mater. Sci., (in press).

10. R.T. Coverdale, B.J. Christensen, T.O. Mason, H.M. Jennings, and E.J. Garboczi "Interpretation of the Impedance Spectroscopy of Cement Paste Via Computer Modelling II: Dielectric Response," J. Mater. Sci.29, 4984 (1994).

11. R.A. Olson, B.J. Christensen, Coverdale, R.T., S.J. Ford, E.J. Garboczi, H.M. Jennings, and T.O. Mason, "Interpretation of the Impedance Spectroscopy of Cement Paste Via Computer Modelling III: Microstructural Analysis of Frozen Cement Paste," submitted to J. Mater. Sci.

12. E.J. Garboczi, "Permeability, Diffusivity, and Microstructural Parameters: A Critical Review," Cem. Concr. Res., Volume 20[4] 591-601 (1990).

13. E.J. Garboczi and D.P. Bentz, "Computer Simulation of the Diffusivity of Cement-Based Materials," J. Mater. Sci., 27, 2083-92 (1992).

14. A.J. Katz and A.H. Thompson, "Quantitative Prediction of Permeability in Porous Rock," Phys. Rev. B, 34[11] 8179-81, (1986).

15. A.J. Moulson and J.M Herbert, Electroceramics, Chapman and Hall, New York, pp. (1990).

16. B.A. Boukamp, Equivalent Circuit (EQUIVCRT.PAS), University of Twente, Department of Chemical Technology, P.O. Box 217, 7500 AE Enschede, The Netherlands, 1988.

17. R.S. Barneyback Jr. and S. Diamond, "Expression and Analysis of Pore Fluids from Hardened Cement Pastes," Cem. Concr. Res., 11, 279-85, (1981).

18. A. Katz, A.R. Brough, T. Bekharev, R.J. Kirkpatrick, L.J. Struble, J.F. Young, "LLW Solidification in Cement - Effect of Dilution," Mat. Res. Soc. Proc., (1994).

19. A.L.A. Fraay, J.M. Bijen, and Y.M. de Hann, "The Reaction of Fly Ash in Concrete. A Critical Examination," Cem. Concr. Res., Vol. 19[2] 235-46 (1989).

20. J. Bijen and H. Pietersen, "Mineral Admixtures: Reactions, Micro-Structure and Macro-Properties," Adv. Cem. Concr.,

21. B.K. Nyame and J.M. Illston, "Capillary Pore Structure and Permeability of Hardened Cement Paste," 7th Intl. Congr. of Cem. Chem., 3, VI181-5 (1980).

22. B.K. Nyame and J.M. Illston, "Relationships Between Permeability and Pore Structure of Hardened Cement Paste," Mag. Concr. Res., 33 (116), 139-46 (1981).

23. N. Banthia and S. Mindess, "Water Permeability of Cement Paste," Cem. Concr. Res., Vol. 19[5] 727-36 (1989).

FIGURES

Figure 1: Temperature schedule for the four different heat treatments. The heavy solid line represents the adiabatic condition.

Figure 2: pH vs. mL HNO_3 used for the titration of the extracted pore solutions of the sample adiabatically cured. Pore solution dilution factor x 100. Figure 2(a) shows the same plot for the original waste solution.

Figure 3: Total alkalinity vs. time as expressed in term of [OH] equivalents of the sample adiabatically cured. Figure 3a is the same plot up to 2 hours.

Figure 4: The variations of the pH vs. time of the extracted pore solution from the sample adiabatically cured.

Figure 5: The variations of the concentrations of Na, K, P, and Al up to 10 h of the pore solution of the pastes cured at 55, 70, and 90C.

Figure 6: The variations of the concentrations of Na, K, Ca, Al, Si, and S up to 30 days of the paste adiabatically cured.

Figure 7: One-day X-ray pattern of the paste cured at 55C. The following denotes: A=alite, ap=apatite, C=$CaCO_3$, H=hemicarbonate, Mu=mullite, Q=quartz, and Z=zeolite.

Figure 8: X-ray patterns of pastes cured at 90C. The following denotes: ap=apatite, C=$CaCO_3$, CH=$Ca(OH)_2$, G=gypsum, H=hemicarbonate, M=monosulfate, Q=quartz, and Z=zeolite.

Figure 9: The normalized conductivity vs. time for the pastes cured at 55, 70, and 85C and that of plain portland cement paste of w/c = 0.5.

Figure 10: A comparison of the calculated and measured permeabilities of various pastes.

Figure 11: Effective dielectric constant vs. time for the pastes cured at 55, 70, and 85C.

FIGURE 1

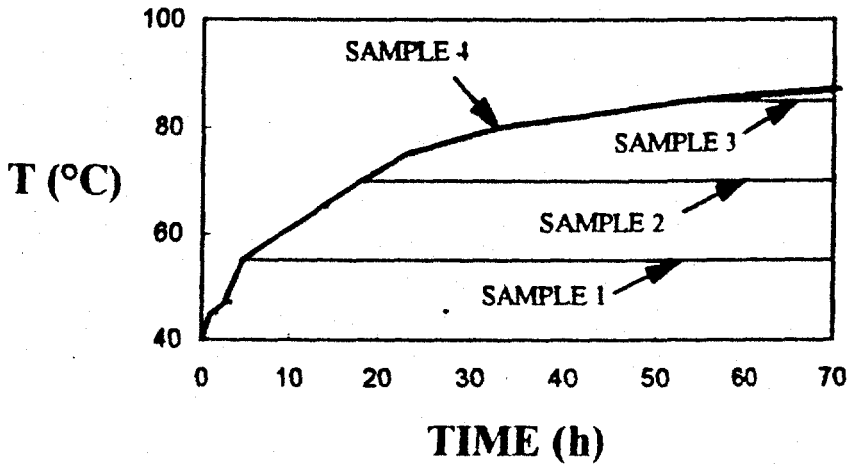
100
80
60
40
T (°C)
SAMPLE 4
SAMPLE 3
SAMPLE 2
SAMPLE 1
0
10
20
30
40
50
60
70
TIME (h)

FIGURE 2

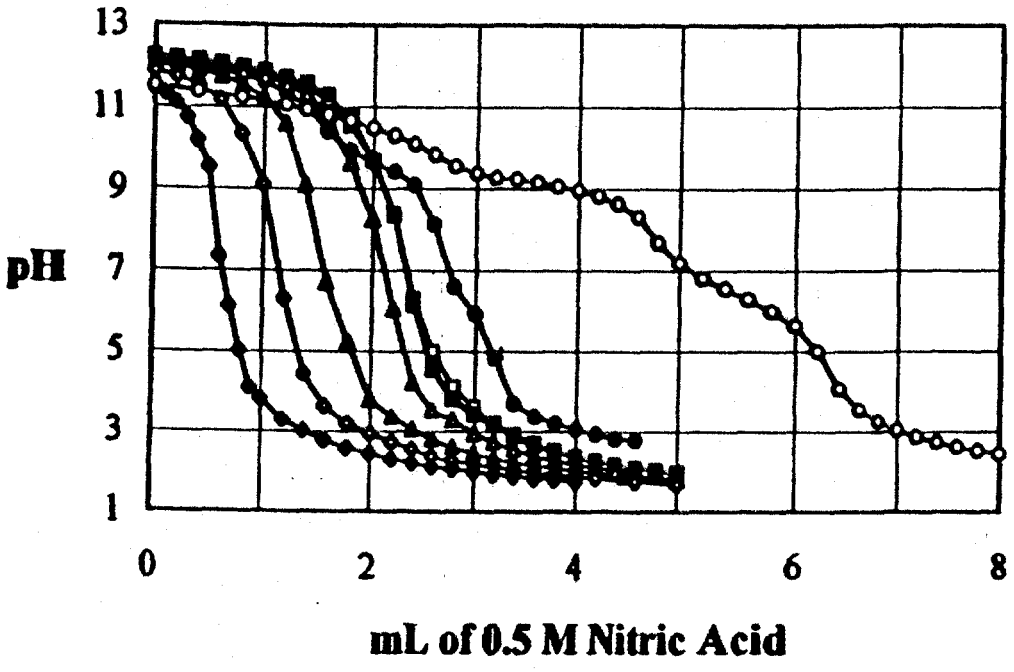

(open circles) waste solution, (filled circles) 0.2 h, (open squares) 1 h, (filled squares) 6 h, (open triangles) 9 h, (filled triangles) 16 h, (open diamonds) 21 h, (filled diamonds) 28 h.

FIGURE 3

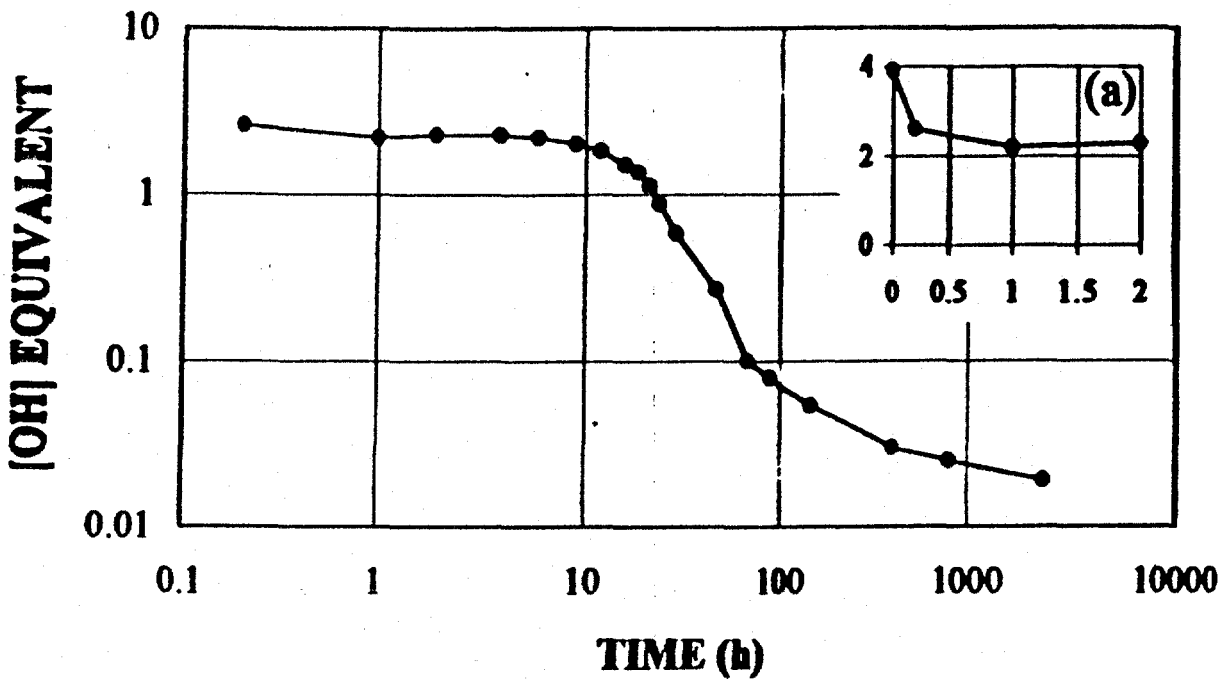
10
1
0.1
0.01
[OH] EQUIVALENT
0.1
1
10
100
1000
10000
TIME (h)
4
2
0
(a)
0
0.5
1
1.5
2

FIGURE 4

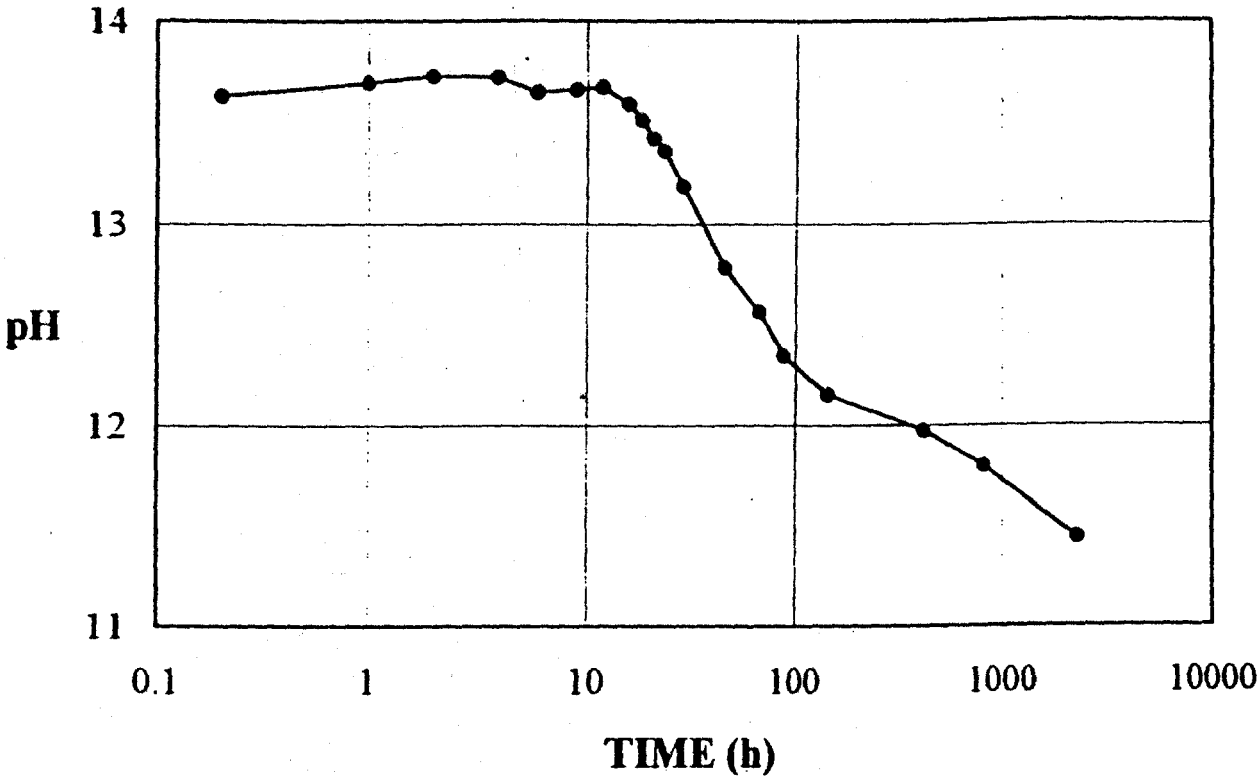

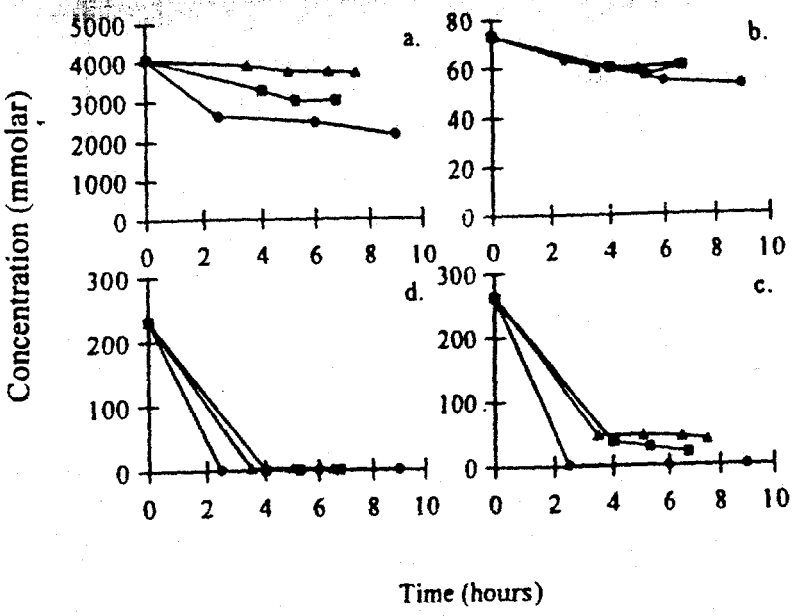

Figure 5. a. Sodium, b. Potassium, c. Phosphorous, d. Aluminum.
Triangles represent samples cured at 55 degrees C, squares 70 deg, and circles 90 deg.

FIGURE 6

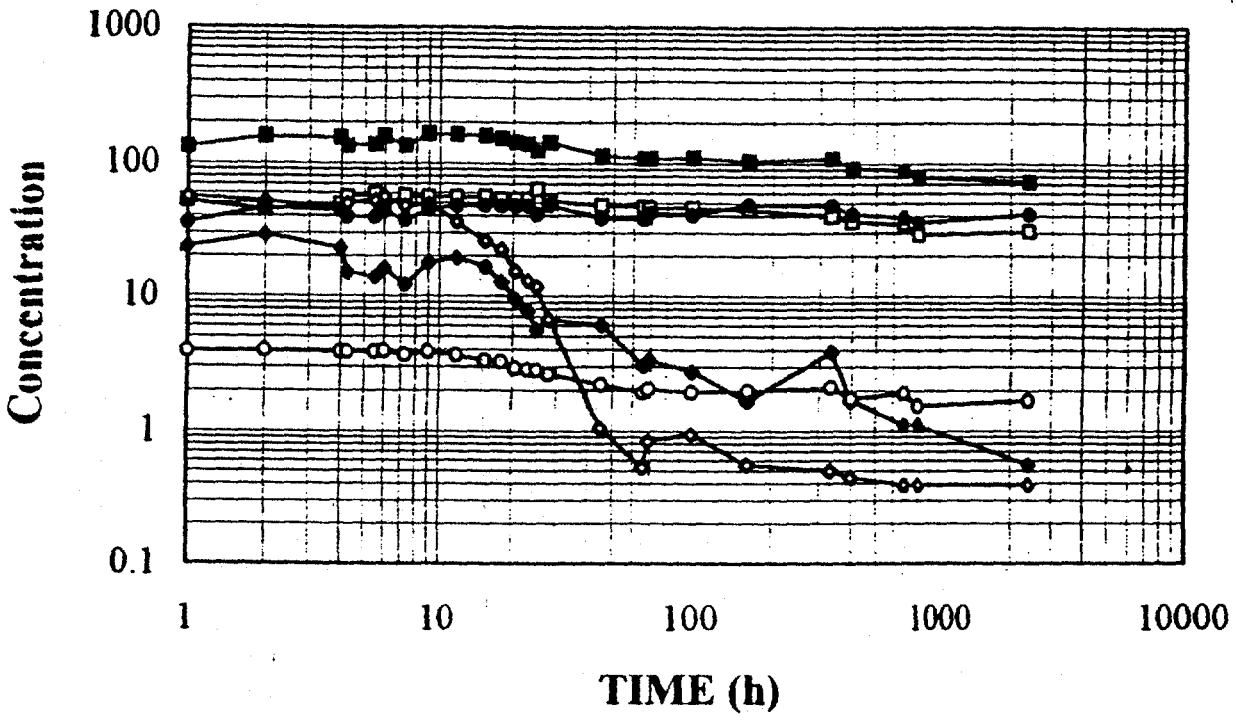

Na (open circles), K (open squares), Ca (filled circles), Al (open diamonds), Si (filled diamonds), S (filled squares).

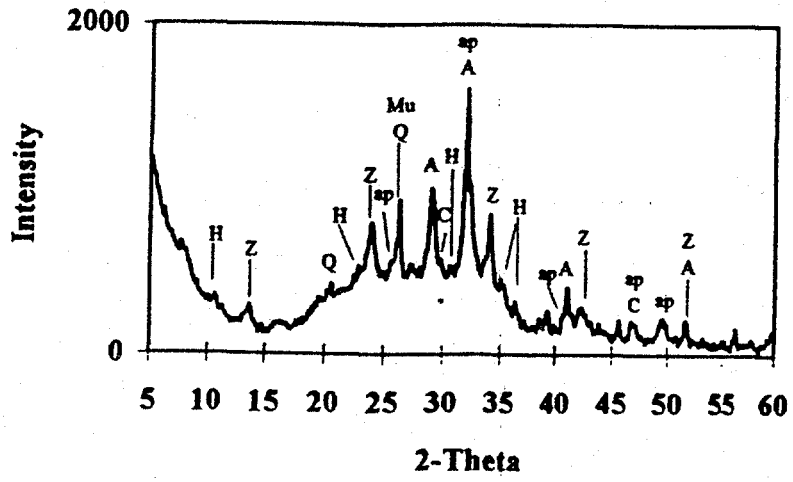
2000
0
Intensity
5 10 15 20 25 30 35 40 45 50 55 60
2-Theta
H
Z
Q
H
Z
sp
Mu
Q
A
H
C
sp
A
Z
H
sp
A
Z
sp
C
sp
Z
A

Figure 7.

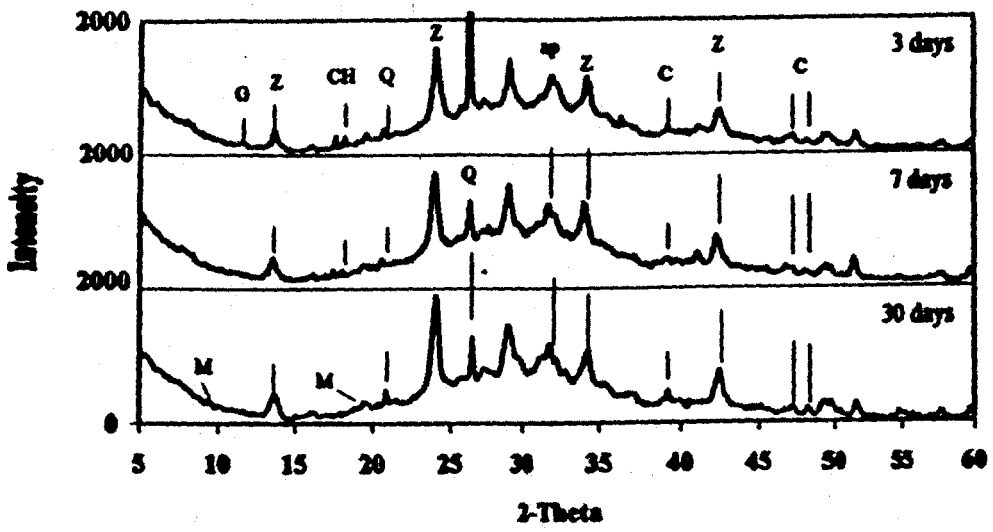
2000
2000
2000
0
Intensity
3 days
7 days
30 days
Z
Q
CH
Z
C
M
5
10
15
20
25
30
35
40
45
50
55
60
2-Theta

Figure 8.

FIGURE 9

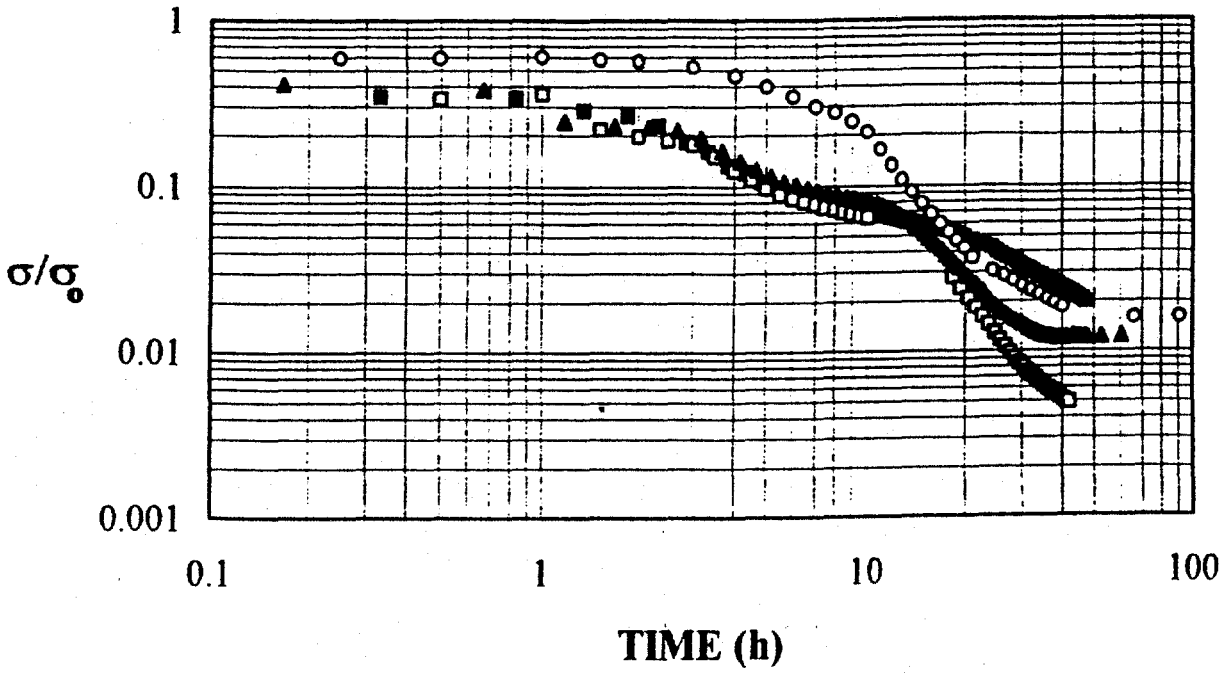

55 C (filled squares), 70 C (open squares), 85 C (filled triangles), plain cement paste w/c = 0.5 (open circles).

FIGURE 10

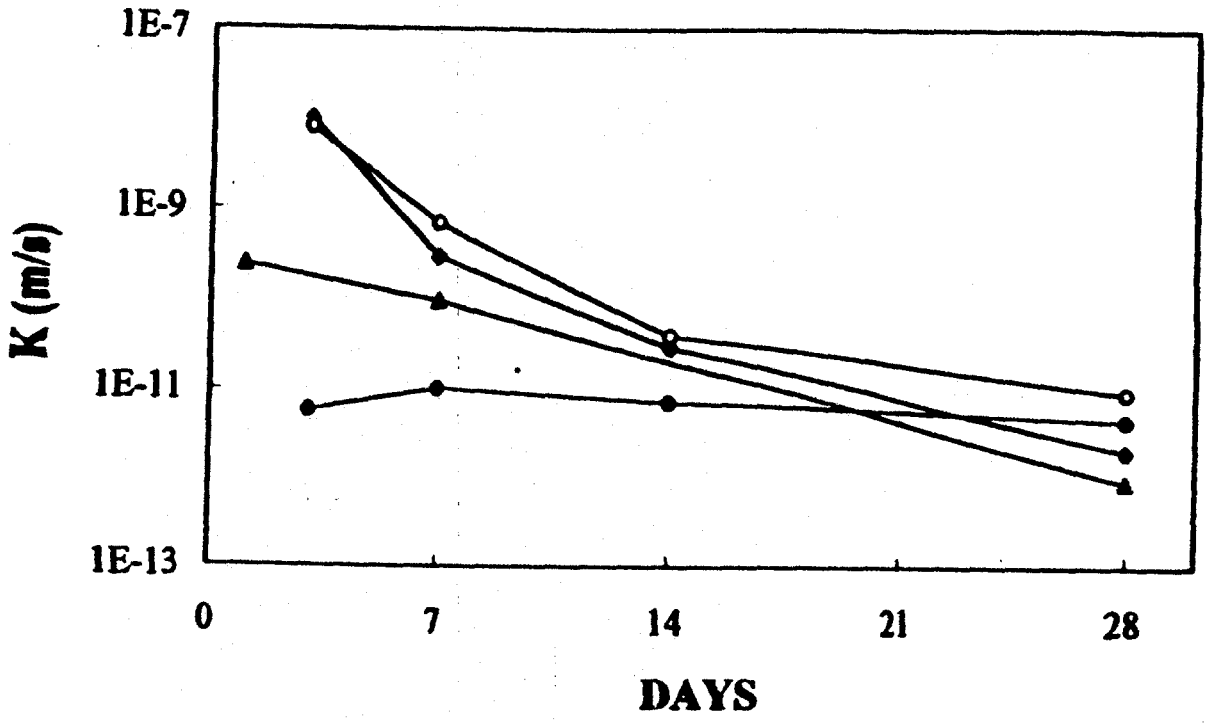

(filled diamonds) Nyame and Illiston, w/c = 0.47, (open circles) Christensen, w/c = 0.47, (filled triangles) Banthia and Mindess, w/c = 0.35, (filled circles) Cement-based waste, s/s = 1.0.

FIGURE 11

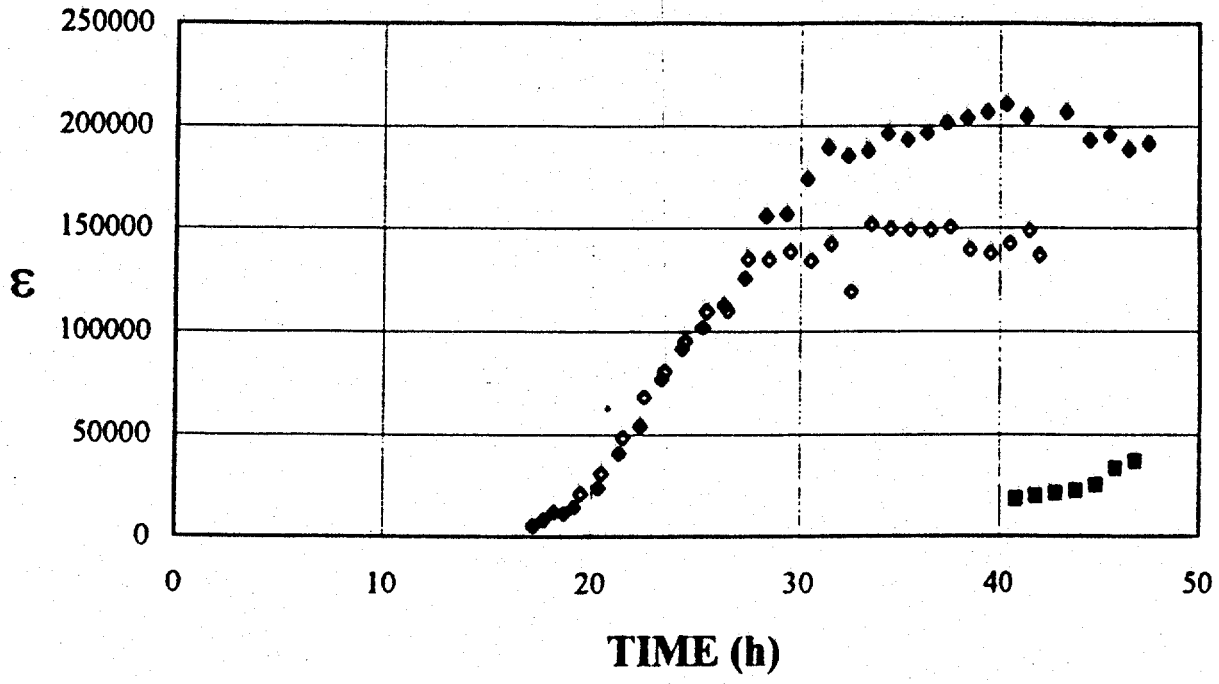

55 C (filled squares), 70 C (open diamonds), and 85 C (filled diamonds).